The Iranian Journal of Mechanical Engineering Transactions of ISME
Journal homepage: https://jmee.isme.ir/
Vol. 25, No. 2, 2024, pp. 26-39

Research Paper

DOI: https://doi.org/10.30506/jmee.2024.2020103.1338

Topology Optimization of Triply Periodic Minimal Surfaces Subjected to Uniaxial Compressive Load

Hosein Geramizadeh[*]
M.Sc.

Sattar Jedari Salami[†]
Associate Professor

Soheil Dariushi[‡]
Associate Professor

Triply periodic minimal surfaces (TPMS) are a class of minimal surfaces that extend along all axes of a Cartesian coordinate system. These surfaces, constructed using trigonometric functions such as sine and cosine, encompass various structures including Gyroid, Schwarz P/D, Neovius, Split P, and Lidinoid. This study focuses on optimizing the topology of the three TPMS-based structures (Neovius, Split P, Schwarz D) for the first time. ABAQUS software and the TOSCA solver were utilized for simulations and optimizations, with a 10% volume fraction constraint, and strain energy is deemed as the objective function. The results demonstrate significant enhancements in the energy absorption capacity of the optimized Neovius, Split P, and Schwarz D structures by approximately 35.72%, 19.06%, and 26.01%, respectively.

Keywords: Triply periodic minimal surface, Neovius, Split P, Schwarz D, Topology optimization, Energy absorption capacity

1 Introduction

Triply periodic minimal surfaces (TPMS) represent fascinating structures in the realm of mechanical engineering, embodying intricate geometrical configurations that extend across all axes of a Cartesian coordinate system: a TPMS consists of unit cells, which are consecutively placed in three independent directions. These surfaces are defined by their fundamental property of being minimal, meaning they achieve surfaces of the least area while spanning the given space. The discovery of TPMS structures dates back to the late 19th century when Schwarz, in collaboration with his student Neovius, laid the foundational groundwork for understanding these geometric wonders [1], [2].

[*]M.Sc., Department of Mechanical Engineering, Central Tehran Branch, Islamic Azad University, Tehran, Iran, hos.geramizadeh.eng@iauctb.ac.ir

[†]Corresponding author, Associate Professor, Department of Mechanical Engineering, Central Tehran Branch, Islamic Azad University, Tehran, Iran, sattar.salami@aut.ac.ir

[‡]Associate Professor, Department of Composite, Faculty of Processing, Iran Polymer and Petrochemical Institute, Tehran, Iran, s.dariushi@ippi.ac.ir

Received: 2023/03/19, Revised: 2023/05/11, Accepted: 2023/09/23

Their pioneering work introduced the first concept of TPMS in 1868, setting the stage for a captivating journey into the world of minimal surfaces [3], [4].
Building upon Schwarz and Neovius's groundwork, the TPMS landscape expanded significantly when Schoen unveiled an additional twelve TPMS variants in 1970 [5]. Schoen's contributions add depth to understanding the evolution of these structures over time. These surfaces, characterized by unit cells arranged systematically along three independent axes, have since captured the imaginations of mathematicians, physicists, material scientists, and engineers alike [6]. The mathematical functions of TPMS generation shed light on the intricate processes behind their formation, showcasing the elegance of trigonometric functions in defining these complex surfaces. These trigonometric functions, utilizing sine and cosine functions, are employed to define surfaces that intricately weave through space without self-intersections. The range of their variables is from $-\pi$ to π for one unit cell. Elaborating on the functional diversity and real-world applications of TPMS structures highlights their broad utility across various fields.TPMS structures, by virtue of their unique geometry, exhibit a mesmerizing range of properties and functionalities [7], [8]. One notable trait is their ability to mimic complex structures found in natural systems, ranging from biological membranes to geological formations. These structures display a remarkable combination of mechanical properties, such as negative Poisson's ratio, exceptional energy absorption capabilities, remarkable stiffness-to-weight ratios, increased lateral surface area, and substantial porosity [9]–[12].
The negative Poisson ratio exhibited by certain TPMS structures is particularly intriguing. Unlike conventional materials, when subjected to tension, these structures expand laterally an anomaly that defies typical material behavior. This property has led to significant interest in utilizing TPMS structures in various fields, especially in the design and development of innovative materials and structures for diverse applications [13]–[15].
One of the most captivating aspects of TPMS structures is their porous nature, which presents an incredibly high surface area relative to their volume. This high surface-to-volume ratio holds immense promise for applications in fields like filtration and tissue engineering, where increased surface area can significantly impact functionality and efficiency [16], [17]. Despite their inherently fascinating properties, TPMS structures continue to intrigue researchers and scientists due to their potential for further optimization and enhancement. By leveraging advanced computational tools and innovative methodologies such as topology optimization, there exists a tremendous opportunity to fine-tune these structures, unlocking even more remarkable mechanical and functional attributes [18], [19].
The optimization of TPMS structures, particularly in terms of topology and geometry, stands as an exciting frontier in materials engineering and computational design [20]. Topology optimization, a powerful numerical technique, focuses on redistributing material within a defined design space to optimize specific performance metrics while adhering to given constraints. In the case of TPMS structures, topology optimization presents a novel approach for enhancing mechanical properties, including but not limited to energy absorption capacities, structural stability, and load-bearing capabilities [21]–[24].
In recent years, significant strides have been made in the computational modeling and optimization of TPMS structures. Researchers have employed sophisticated software tools and algorithms to explore the vast design space of these structures, seeking optimal configurations that maximize performance metrics. This includes exploring novel unit cell arrangements, refining surface geometries, and investigating intricate lattice configurations to achieve superior mechanical and functional properties [25], [26]. Furthermore, the quest to optimize TPMS structures aligns seamlessly with the broader paradigm of material science and engineering wherein the quest for novel materials and structures with enhanced performance characteristics remains a central focus. The potential applications of optimized TPMS structures span across diverse sectors, ranging from aerospace and automotive industries to biomedical engineering and beyond [27].

Table 1 Mechanical properties of the ABS polymeric filament

Material model	Elastic		Plastic			
	Young's modulus (*Mpa*)	Poisson's ratio	A (*Mpa*)	B (*Mpa*)	n	m
Johnson-Cook	1680±10	0.35	108.24±5	248.14±5	11.03	0

Therefore, understanding and optimizing TPMS structures hold immense promise in advancing technological frontiers and addressing complex challenges in various industries [2].
This study focuses on presenting a new approach for optimizing the topology of three distinct TPMS structures (Neovius, Split P, and Schwarz D). The main aim is to reveal novel configurations that exhibit enhanced mechanical properties, particularly in terms of energy absorption capacities. Leveraging advanced computational tools and simulation techniques, this work endeavors to pioneer new insights into optimizing TPMS structures, thereby contributing to the broader landscape of materials engineering and computational design. Moreover, by harnessing the inherent intricacies of TPMS geometries through optimization, this study endeavors to offer innovative solutions that transcend conventional material limitations, fostering new possibilities in materials science and engineering applications. The current meticulous investigation seeks to unravel the untapped potential of TPMS structures, unlocking novel configurations that push the boundaries of mechanical performance, functional versatility, and design innovation.

2 Material and methods

2.1 Mechanical properties characterization

In this study, the mechanical properties of the Acrylonitrile Butadiene Styrene (ABS) filament based on the standard ASTM D695-15, which were derived from the authors' previous investigations [28]–[30]. This filament serves as an ideal candidate for understanding the mechanical behavior of polymeric materials commonly used in various engineering applications. The polymeric material was characterized by employing the widely recognized Johnson-Cook material model.
The Johnson-Cook material model is highly relevant in this study due to its capability to capture the complex mechanical response of polymeric materials, such as ABS filaments. The Johnson-Cook model, known for its efficacy in capturing the complex material response under varying strain rates, encompasses key parameters such as Young's modulus, Poisson's ratio, and material constants (A, B, n, and m), which are mentioned in Table (1). These parameters were meticulously determined through curve-fitting techniques applied to the experimental stress-strain data of the ABS filament. This filament, being commonly used in various engineering applications, holds significant implications for understanding and predicting the mechanical behavior of polymeric materials. The resulting material model aimed to accurately represent the mechanical behavior of the ABS material, crucial for subsequent numerical simulations and structural analyses.

2.2 Triply periodic minimal surface modeling

The central focus of this investigation revolved around three distinct TPMS models (Neovius, Split P, and Schwarz D) each embodying unique geometric characteristics and structural complexities. The generation and formulation of these TPMS structures were meticulously conducted using advanced computational tools and techniques.

MATLAB R2015b, a powerful numerical computing environment, served as the primary platform for the generation of these intricate structures. Also, this computing environment is widely used for its mathematical algorithms and programming functionalities. The Neovius, Split P, and Schwarz D models were constructed based on Eqs. (1), (2), and (3), respectively, which are mentioned as follows (see Appendixes).

$$3(\cos x + \cos y + \cos z) + 4(\cos x \times \cos y \times \cos z) = 0 \tag{1}$$

$$\begin{aligned} 1.1(\sin 2x \times \cos y \times \sin z + \sin 2y \times \cos z \times \sin x + \sin 2z \times \cos x \times \sin y) \\ - 0.2(\cos 2x \times \cos 2y + \cos 2y \times \cos 2z + \cos 2z \times \cos 2x) \\ - 0.4(\cos 2x + \cos 2y + \cos 2z) = 0 \end{aligned} \tag{2}$$

$$\begin{aligned} (\sin x \times \sin y \times \sin z) + (\sin x \times \cos y \times \cos z) + (\cos x \times \sin y \times \cos z) \\ + (\cos x \times \cos y \times \sin z) = 0 \end{aligned} \tag{3}$$

These equations, rooted in trigonometric functions, including sine and cosine, allowed for the precise generation and visualization of the intricate surfaces comprising these TPMS structures. The range of their variables is from -2π to 2π for 2 unit cells. Each TPMS model was meticulously designed to consist of 2 × 2 × 2 unit cells, facilitating a comprehensive analysis of their mechanical and topological characteristics. These structures were rescaled from 12.56 *mm* to 10 *mm* in CATIA software in order to have integer dimensions.

The dimensions of these TPMS structures, comprising height (*H*), length (*L*), and width (*W*), were defined to achieve consistency and relevance in the ensuing simulations and analyses. The dimensions were chosen strategically to ensure a coherent representation of the TPMS structures within the computational framework. These dimensions are graphically illustrated and mentioned in Figure (1) and Table (2), respectively. The thickness of Neovius, Split P, and Schwarz D was taken equal to 0.43382 *mm*, 0.297006 *mm*, and 0.19818 *mm*, respectively, to consider them in the same relative density (30%).

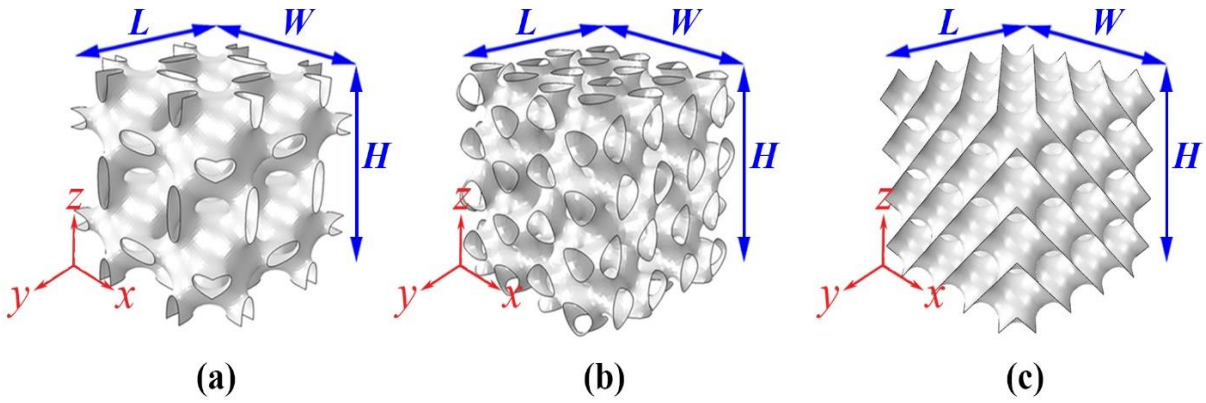

Figure 1 Models of TPMS structures created in MATLAB **a**) Neovius, **b**) Split P and **c**) Schwarz D

Table 2 Dimensions of the structures (*mm*)

TPMS	*H*	*L*	*W*
Neovius	10	10	10
Split P	10	10	10
Schwarz D	10	10	10

2.3 Material model implementation in computational simulations

The computational simulations conducted in this study necessitated the integration and utilization of the previously established Johnson-Cook material model within the numerical framework. This involved the meticulous incorporation of the derived material parameters including Young's modulus, Poisson's ratio, and the material constants (A, B, n, and m) into the computational models utilized for structural analyses.
The ABAQUS software, renowned for its versatility in conducting finite element simulations and structural analyses, served as the primary computational tool for implementing numerical investigations. The ABS material model derived through the Johnson-Cook formulation was integrated into the computational domain within ABAQUS. This integration involved defining the material properties, constitutive laws, and material behavior models within the computational framework to accurately emulate the mechanical response of the ABS material under various loading conditions.

2.4 Energy absorption capacity and Its growth rate

Energy absorption capacity (U) plays a pivotal role in evaluating the mechanical performance of a structure subjected to uniaxial compressive and tensile load. This dependent scaler quantity has direct and inverse relations with absorbed energy and volume, respectively, which is expressed by

$$U = \frac{\int_0^{\delta} F(x)dx}{V} \tag{4}$$

where $F(x)$, x, and V are reaction force, displacement, and volume, respectively. The amounts of variable, δ, were equal to 0.2 *mm* (strain 4%). In the optimization process, the growth rate of energy absorption capacity is a comparative quantity indicating the percentage of improvement in structures' mechanical behavior under the same boundary conditions.

2.5 Mesh generation and convergence studies

A crucial aspect of ensuring the accuracy and reliability of numerical simulations lies in the generation of high-quality meshes that accurately represent the geometry and intricacies of the TPMS structures. To achieve this, a meticulous mesh generation process was undertaken utilizing the ABAQUS software platform. The TPMS models (Neovius, Split P, and Schwarz D) were subjected to a rigorous meshing procedure employing finite element meshing techniques.
Various mesh parameters, including element sizes, element types, and mesh densities, were adjusted and optimized to achieve mesh convergence, wherein the numerical solutions exhibit consistent behavior and accuracy with refined mesh resolutions. Convergence studies were conducted, involving the systematic refinement of mesh parameters and analyses of the resultant solutions to ascertain convergence criteria.
The convergence of numerical solutions was assessed through a meticulous examination of solution sensitivities to mesh refinements. This involved conducting multiple simulations with varying mesh resolutions and assessing the stability and consistency of the obtained results. Upon achieving convergence, where subsequent mesh refinements yielded negligible changes in the solutions, the optimum mesh configuration was identified for each TPMS structure, ensuring accuracy and reliability in subsequent simulations. The models were meshed by the 3-node triangular general-purpose shell, finite membrane strains (S3).

2.6 Boundary conditions and loading configurations

The computational simulations entailed the imposition of realistic boundary conditions and loading configurations to emulate real-world structural responses of the TPMS models under the uniaxial compressive test. Consideration was given to defining appropriate boundary conditions that accurately represented the structural constraints and interactions within the computational domain. Furthermore, two rigid planes with a reference point were created as simple supports. As illustrated in Figure (2), these rigid planes were strategically positioned relative to the TPMS structures to ensure stability and structural integrity during the simulated loading conditions. A finite uniaxial displacement, which was equal to 0.6 *mm*, was allocated to the upper reference point, and all degrees of freedom were taken from the bottom one. In the interaction module, two contacts with a 0.3 friction coefficient were defined between the up/down edges and planes. Furthermore, loading configurations were defined to replicate realistic loading conditions experienced by these structures. Uniaxial loading, simulating compressive loading was applied to the TPMS structures to assess their mechanical response under uniaxial compression. The loading conditions were carefully calibrated to achieve desired strain levels and assess the structural behavior and mechanical performance of the TPMS models.

2.7 Optimization procedure and algorithm implementation

The main aim of this work is to optimize the topology of Neovius, Split P, and Schwarz D structures to enhance their mechanical properties, particularly focusing on their energy absorption capacities. To achieve this purpose, a sophisticated optimization procedure leveraging topology optimization methodologies was implemented.

TOSCA, a specialized optimization solver known for its efficacy in conducting topology optimization studies, is employed in conjunction with the ABAQUS software. The optimization algorithm utilized within the TOSCA solver employed iterative optimization techniques to alleviate the elements on which the von Mises stresses are less concentrated. In order to preserve elements that were exposed to boundary conditions and structural stability, two sections with a distance of 1 *mm* from the top and bottom edges of the TPMS models were restricted as frozen areas, considering that the frozen elements remained intact during the topology optimization process.

Figure (3) shows these regions, which are highlighted in transparent red color.

In this investigation, volume fraction and strain energy were selected as design responses to the topology optimization process. One of the design responses is the objective function which is defined to maximize the strain energy, also the other one is allocated to constrain focusing on minimizing the volume.

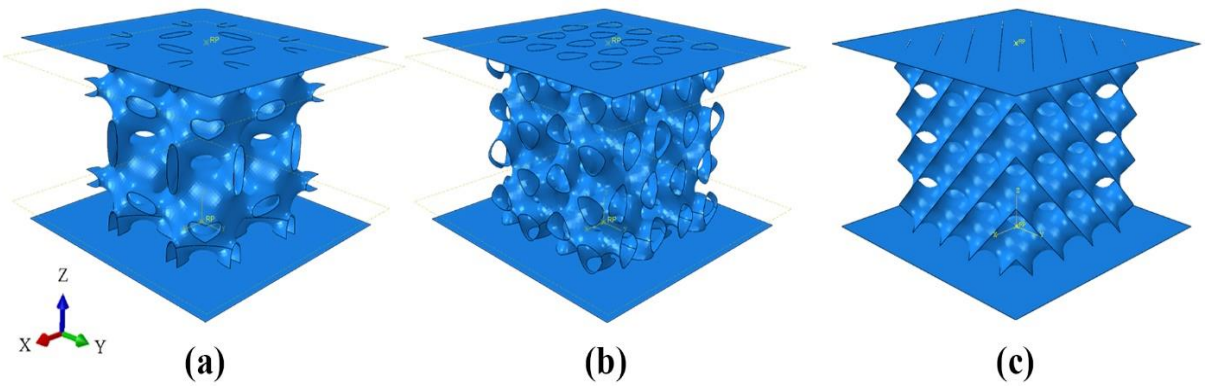

Figure 2 Imported shell models in assemble module **a**) Neovius, **b**) Split P and **c**) Schwarz D

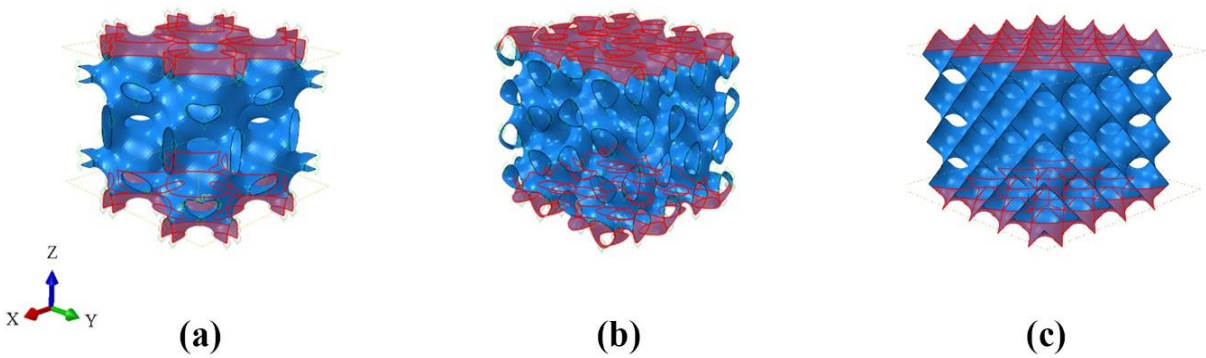

Figure 3 Restricted regions **a**) Neovius, **b**) Split P and **c**) Schwarz D

In each optimization step, the constraint was decreased by 10% of the initial model's volume, and the energy absorption capacity of each optimized model was determined and compared. The volume reduction continues along the optimization process until the energy absorption capacity is optimized.

3 Results and discussions

3.1 Numerical validation

In order to validate the numerical procedure, the results were compared with another study [31] on the Schwarz D simulated based on the same material model. The comparison revealed a slight difference of 0.02% in the numerical elastic modulus between the current investigation (E) and the other study (E^*) [31]. Table 3 illustrates the elastic modulus of the Schwarz D models under the same boundary conditions. According to the comparison, it can be deduced the numerical results are verified.

3.2 Mesh and optimization convergence

Mesh convergence was separately implemented for each model. As shown in Figure (4 (a)), the slope of the approximate global mesh size decreased as the number of elements increased to the point where it became almost horizontal. Additionally, the same trend occurred in the reaction force curve, which means the appropriate number of elements was obtained. In optimization convergence, which is indicated in Figure (4 (b)), optimization convergence was successfully performed, considering that both design responses reached their target in the same cycle.

3.3 Compressive simulations and stress distributions

The comprehensive computational simulations conducted on Neovius, Split P, and Schwarz D structures provided profound insights into their mechanical responses under uniaxial compressive loading conditions. As shown in Figure (5), von Mises stress distributions within these structures unveiled intricate stress concentration patterns, shedding light on their mechanical behaviors. In the Neovius structure, the von Mises stress contours showcased prominent stress concentrations primarily along the loading axis (Z-direction), indicating localized regions experiencing significantly higher stress levels.

Table 3 Comparison between numerical elastic modulus of the Schwarz D models (MPa)

TPMS	E^*	E
Schwarz D	102	101.98

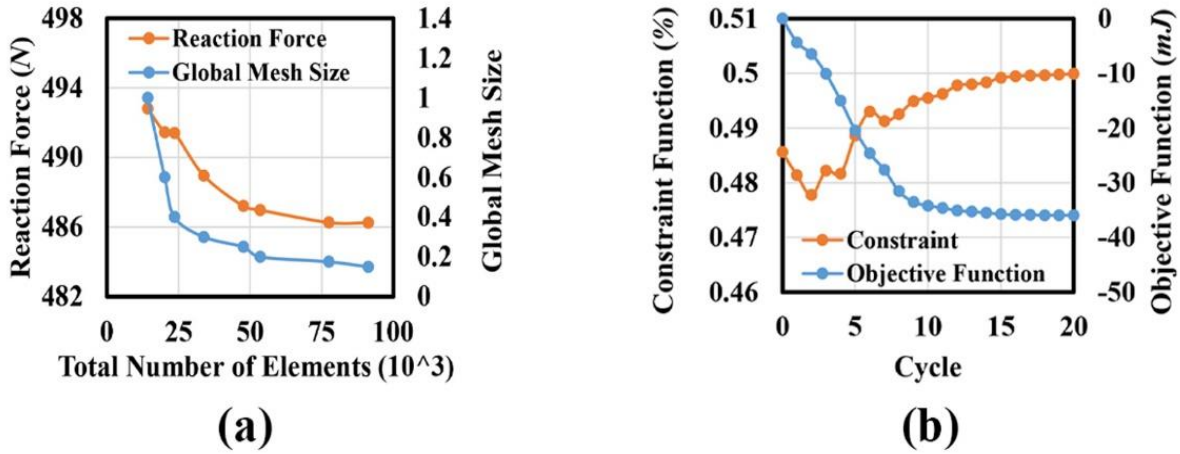

Figure 4 Simulation and optimization for Neovius at strain 4% **a**) Mesh convergence and **b**) Optimization convergence

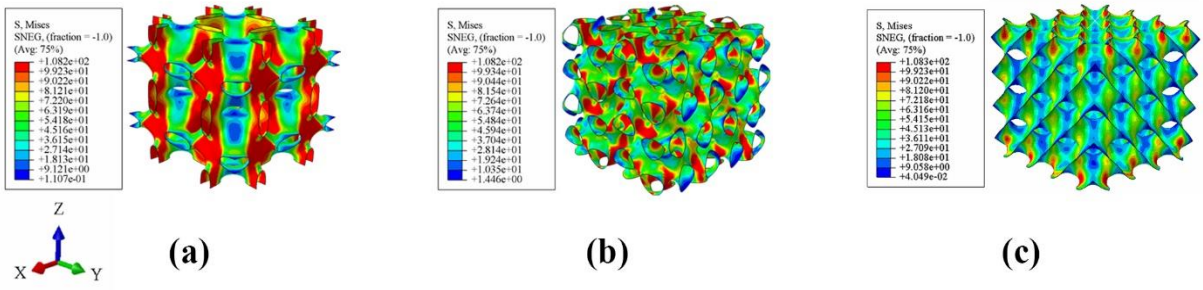

Figure 5 The von Mises stress contours **a**) Neovius, **b**) Split P and **c**) Schwarz D

These stress concentrations were attributed to the geometrical intricacies within the Neovius structure, specifically the interconnected channels and porous features, leading to localized stress accumulations along certain pathways.

Conversely, the Split P structure exhibited a contrasting stress distribution pattern. The von Mises stress contours in Split P revealed a more uniform stress distribution across the structure compared to Neovius. This uniform stress dispersion could be attributed to the distinctive geometric configuration of Split P, characterized by interconnected surfaces and distinct channels, resulting in a more balanced stress distribution throughout the structure.

The stress distributions observed within the Schwarz D structure exhibited intermediate characteristics between Neovius and Split P. The stress contours demonstrated localized stress concentrations akin to Neovius, albeit with a comparatively more dispersed stress pattern across the structure, reminiscent of Split P. This unique stress distribution profile in Schwarz D indicated a blend of localized stress concentrations and a more balanced stress dispersion compared to Neovius and Split P.

3.4 Energy absorption capacity and optimization outcomes

The central focus of this study was to optimize the topology of Neovius, Split P, and Schwarz D TPMS structures to enhance their energy absorption capacities, which are demonstrated in Figure (6). The optimization process, conducted using sophisticated algorithms within the TOSCA optimization framework, aimed to refine the structural configurations iteratively and achieve optimal designs.

Results from the optimization process revealed notable enhancements in the energy absorption capacities of the optimized TPMS structures.

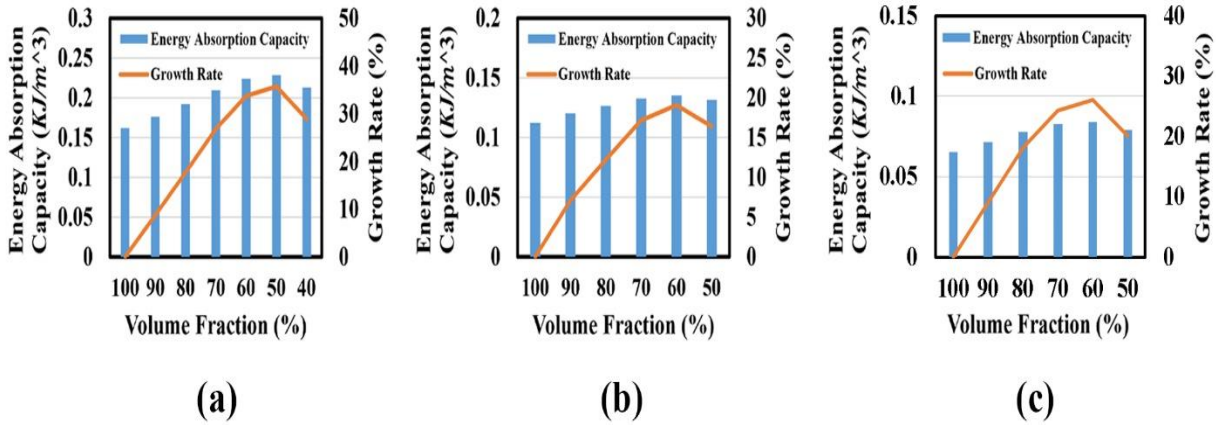

Figure 6 Comparison among energy absorption capacities and its growth rates **a**) Neovius, **b**) Split P and **c**) Schwarz D

Specifically, the optimized Neovius structure exhibited a remarkable increase in energy absorption capacity, showcasing an improvement from an initial value of 162.07 J/m^3 to an optimized value of 228.46 J/m^3. This significant enhancement in energy absorption capacity highlighted the efficacy of topology optimization in refining the structural configurations of Neovius, enabling it to better withstand and dissipate mechanical loads.

Similarly, the optimization of the Split P structure yielded substantial improvements in energy absorption capacity. The initial energy absorption capacity of Split P stood at 112.3 J/m^3, which was significantly enhanced to 131.57 J/m^3 through the topology optimization process. This enhancement underscored the ability of topology optimization to strategically modify the topology of Split P, resulting in improved mechanical performance and energy dissipation capabilities.

The optimization outcomes for the Schwarz D structure also demonstrated considerable improvements in energy absorption capacity. The initial energy absorption capacity of Schwarz D was systematically refined through topology optimization, elevating it from an initial value of 65.41 $J/m^3$to a significantly enhanced value of 84.29 J/m^3. This enhancement in energy absorption capacity indicated the potential of topology optimization methodologies in tailoring the structural configurations of Schwarz D to achieve superior mechanical performance under compressive loading conditions.

3.5 Comparison among optimization outputs

As illustrated in Table (4), comparative analysis among the optimization outputs of Neovius, Split P, and Schwarz D structures disclosed distinct structural configurations and performance characteristics. The optimized Neovius structure exhibited superior energy absorption capacity compared to both Split P and Schwarz D at the corresponding optimized configurations.

Furthermore, a detailed examination of the optimized topologies revealed variations in porosity among the structures. The optimized Neovius structure demonstrated higher porosity compared to both Split P and Schwarz D, indicating a higher surface-to-volume ratio and potential advantages in applications requiring increased surface area.

Moreover, the optimized Split P and Schwarz D structures exhibited intermediate porosity levels, showcasing a balanced distribution of structural elements and pore spaces. These porosity variations among the optimized structures highlighted the influence of topology optimization on the structural configurations and mechanical properties of TPMS structures.

Table 4 Optimized configurations

Volume Fraction	Neovius	Split P	Schwarz D
90%	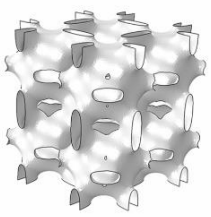	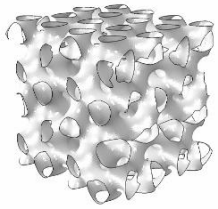	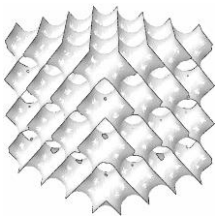
80%	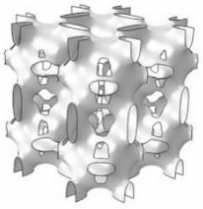	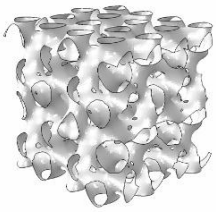	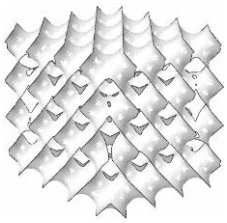
70%	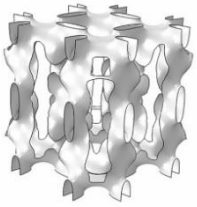	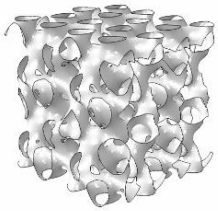	
60%	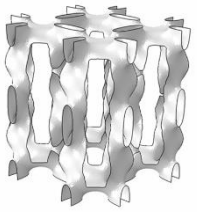	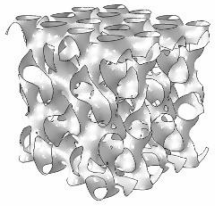	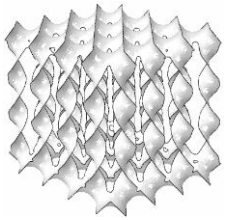
50%	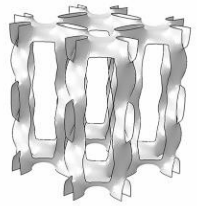	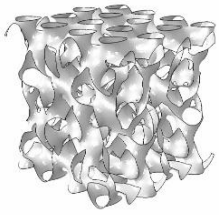	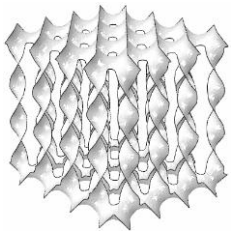
40%	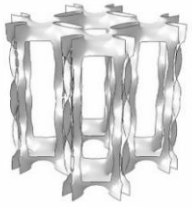		

4 Conclusion

The current study aims to implement comprehensive computational simulations and topology optimization on Neovius, Split P, and Schwarz D structures yielding profound insights into their mechanical performances and optimization potential. This investigation reveals distinctive stress distributions within the structures under compressive loading, emphasizes significant improvements in energy absorption capacities through topology optimization, and highlights the impact of topological modifications on stress dissipations. Moreover, an innovative algorithm for optimizing the topology of shell models is introduced, which has been provided for the first time. Overall, this study showcases the potential of topology optimization to

enhance the mechanical properties of TPMS structures, paving the way for their application in various fields requiring lightweight, high-performance lattice structures. The extracted results are interpreted as follows:

- Computational simulations disclose distinctive stress distribution patterns within Neovius, Split P, and Schwarz D TPMS structures under compressive boundary conditions, illustrating localized stress concentrations and variations in stress dispersion across the structures.
- Topology optimizations significantly enhance energy absorption capacities: Neovius exhibited an increase from 162.07 J/m^3 to 228.46 J/m^3, Split P increased from 112.3 $J/m^3$to 131.57 J/m^3, and Schwarz D showed substantial improvements from 65.41 J/m^3 to 84.29 J/m^3.
- Structural modifications observed in the optimized TPMS models included redistributed material distributions and refined geometrical features, contributing to improved stress dissipation pathways and mitigating stress concentrations.
- Neovius demonstrated superior energy absorption capacity compared to Split P and Schwarz D at corresponding optimized configurations, alongside higher porosity, indicating potential advantages in applications requiring increased surface area.
- The tremendous achievements reveal the efficacy of topology optimization in enhancing the mechanical properties of TPMS structures, presenting promising prospects for diverse industrial applications.

References

[1] H. A. Schwarz, Gesammelte Mathematische Abhandlungen. in AMS Chelsea Publishing Series. Chelsea Publishing Company, 1972. [Online]. Available: https://books.google.co.jp/books?id=cKWBJBcM_18C.

[2] T. Poltue, C. Karuna, S. Khrueaduangkham, S. Seehanam, and P. Promoppatum, “Design Exploration of 3D-printed Triply Periodic Minimal Surface Scaffolds for Bone Implants,“ International Journal of Mechanical Sciences, Vol. 211, p. 106762, 2021, doi: https://doi.org/10.1016/j.ijmecsci.2021.106762.

[3] D. W. Abueidda, M. Bakir, R. K. Abu Al-Rub, J. S. Bergström, N. A. Sobh, and I. Jasiuk, “Mechanical Properties of 3D Printed Polymeric Cellular Materials with Triply Periodic Minimal Surface Architectures,“ Materials & Design, Vol. 122, pp. 255–267, 2017, doi: https://doi.org/10.1016/j.matdes.2017.03.018.

[4] M. Rezapourian, N. Kamboj, and I. Hussainova, “Numerical Study on the Effect of Geometry on Mechanical Behavior of Triply Periodic Minimal Surfaces,“ IOP Conference Series: Materials Science and Engineering, Vol. 1140, No. 1, p. 012038, 2021, doi: https://doi.org/10.1088/1757-899X/1140/1/012038.

[5] A. H. Schoen, “Infinite Periodic Minimal Surfaces without Self-intersections,“, Vol. 5541, United States: National Aeronautics and Space Administration, 1970.

[6] S. AlMahri, R. Santiago, D. Lee, H. Ramos, H. Alabdouli, M. Alteneiji, Z. Guan, and M. Alves, “Investigation of the Specific Energy Absorption of Triply Periodic Minimal Surfaces Subjected to Impact Loading,“ EPJ Web of Conferences, Vol. 250, p. 01022, 2021, doi:

https://doi.org/10.1051/epjconf/202125001022.

[7] V. Nguyen-Van, P. Tran, C. Peng, L. Pham, G. Zhang, and H. Nguyen-Xuan, "Bioinspired Cellular Cementitious Structures for Prefabricated Construction: Hybrid Design & Performance Evaluations," Automation in Construction, Vol. 119, p. 103324, 2020, doi: https://doi.org/10.1016/j.autcon.2020.103324.

[8] R. Asbai-Ghoudan, S. Ruiz de Galarreta, and N. Rodriguez-Florez, "Analytical Model for the Prediction of Permeability of Triply Periodic Minimal Surfaces," Journal of the Mechanical Behavior of Biomedical Materials, Vol. 124, p. 104804, 2021, doi: https://doi.org/10.1016/j.jmbbm.2021.104804.

[9] O. Al-Ketan and R. K. Abu Al-Rub, "Multifunctional Mechanical Metamaterials Based on Triply Periodic Minimal Surface Lattices," Advanced Engineering Materials, Vol. 21, No. 10, 2019, doi: https://doi.org/10.1002/adem.201900524.

[10] J. M. Ashraf, S. E. Taher, D.-W. Lee, K. Liao, and R. K. Abu Al-Rub, "On the Computational Modeling, Additive Manufacturing, and Testing of Tube-networks TPMS-based Graphene Lattices and Characterizing Their Multifunctional Properties," APL Materials, Vol. 10, No. 12, 2022, doi: https://doi.org/10.1063/5.0101412.

[11] C. S. Ha, R. S. Lakes, and M. E. Plesha, "Cubic Negative Stiffness Lattice Structure for Energy Absorption: Numerical and Experimental Studies," International Journal of Solids and Structures, Vol. 178–179, pp. 127–135, 2019, doi: https://doi.org/10.1016/j.ijsolstr.2019.06.024.

[12] T. Wang, J. An, H. He, X. Wen, and X. Xi, "A Novel 3D Impact Energy Absorption Structure with Negative Poisson's Ratio and its Application in Aircraft Crashworthiness," Composite Structures, Vol. 262, p. 113663, 2021, doi: https://doi.org/10.1016/j.compstruct.2021.113663.

[13] Y. Du, J. Maassen, W. Wu, Z. Luo, X. Xu, and P. D. Ye, "Auxetic Black Phosphorus: A 2D Material with Negative Poisson's Ratio," Nano Letters, Vol. 16, No. 10, pp. 6701–6708, 2016, doi: https://doi.org/10.1021/acs.nanolett.6b03607.

[14] J. N. Grima-Cornish, J. N. Grima, and D. Attard, "A Novel Mechanical Metamaterial Exhibiting Auxetic Behavior and Negative Compressibility," Materials, Vol. 13, No. 1, p. 79, 2019, doi: https://doi.org/10.3390/ma13010079.

[15] W. Yang, J. An, C. K. Chua, and K. Zhou, "Acoustic Absorptions of Multifunctional Polymeric Cellular Structures Based on Triply Periodic Minimal Surfaces Fabricated by Stereolithography," Virtual and Physical Prototyping, Vol. 15, No. 2, pp. 242–249, 2020, doi: https://doi.org/10.1080/17452759.2020.1740747.

[16] J. Feng, J. Fu, C. Shang, Z. Lin, and B. Li, "Porous Scaffold Design by Solid T-splines and Triply Periodic Minimal Surfaces," Computer Methods in Applied Mechanics and Engineering, Vol. 336, pp. 333–352, 2018, doi: https://doi.org/10.1016/j.cma.2018.03.007.

[17] J. Feng, J. Fu, X. Yao, and Y. He, "Triply Periodic Minimal Surface (TPMS) Porous Structures: from Multi-scale Design, Precise Additive Manufacturing to Multidisciplinary

Applications," International Journal of Extreme Manufacturing, Vol. 4, No. 2, p. 022001, 2022, doi: https://doi.org/10.1088/2631-7990/ac5be6.

[18] S. Zhang, D. Da, and Y. Wang, "TPMS-infill MMC-based Topology Optimization Considering Overlapped Component Property," International Journal of Mechanical Sciences, Vol. 235, p. 107713, 2022, doi: https://doi.org/10.1016/j.ijmecsci.2022.107713.

[19] I. El Khadiri, M. Abouelmajd, M. Zemzami, N. Hmina, M. Lagache, B. AlMangour, A. Bahlaoui, I. Arroub, and S. Belhouideg, "TPMS Lattice Structure Derived using Topology Optimization for the Design of Additive Manufactured Components,", in *2022 8th International Conference on Optimization and Applications (ICOA)*, IEEE, Oct. 2022, pp. 1–4, . doi: https://doi.org/10.1109/ICOA55659.2022.9934649.

[20] C. Yang and Q. M. Li, "Advanced Lattice Material with High Energy Absorption Based on Topology Optimisation," *Mechanics of Materials*, Vol. 148, p. 103536, 2020, doi: https://doi.org/10.1016/j.mechmat.2020.103536.

[21] J. Hu, S. Wang, B. Li, F. Li, Z. Luo, and L. Liu, "Efficient Representation and Optimization for TPMS-based Porous Structures," *IEEE Transactions on Visualization and Computer Graphics*, Vol. 28, No. 7, pp. 2615–2627, 2022, doi: https://doi.org/10.1109/TVCG.2020.3037697.

[22] A. Viswanath, M. Modrek, K. A. Khan, and R. K. A. AL-Rub, "Deep Learning for Topology Optimization of Triply Periodic Minimal Surface Based Gyroid-like Structures,", in *American Society for Composites 2021*, Destech Publications, Inc., Sep. 2021. doi: https://doi.org/10.12783/asc36/35824.

[23] N. Strömberg, "Optimal Grading of TPMS-based Lattice Structures with Transversely Isotropic Elastic Bulk Properties," *Engineering Optimization*, Vol. 53, No. 11, pp. 1871–1883, 2021, doi: https://doi.org/10.1080/0305215X.2020.1837790.

[24] M. J. Buehler, B. Bettig, and G. G. Parker, "Topology Optimization of Smart Structures using a Homogenization Approach," *Journal of Intelligent Material Systems and Structures*, Vol. 15, No. 8, pp. 655–667, 2004, doi: https://doi.org/10.1177/1045389X04043944.

[25] L. Zhang, S. Feih, S. Daynes, S. Chang, M.Y. Wang, J. Wei, and W.F. Lu "Energy Absorption Characteristics of Metallic Triply Periodic Minimal Surface Sheet Structures under Compressive Loading," *Additive Manufacturing*, Vol. 23pp. 505–515, 2018, doi: https://doi.org/10.1016/j.addma.2018.08.007.

[26] K. Yeranee, Y. Rao, L. Yang, and H. Li, "Improved Thermal Performance of a Serpentine Cooling Channel by Topology Optimization Infilled with Triply Periodic Minimal Surfaces," *Energies*, Vol. 15, No. 23, p. 8924, 2022, doi: https://doi.org/10.3390/en15238924.

[27] N. Novak, O. Al-Ketan, L. Krstulović-Opara, R. Rowshan, R.K.A. Al-Rub, M. Vesenjak, and Z. Ren, "Quasi-static and Dynamic Compressive Behaviour of Sheet TPMS Cellular Structures," *Composite Structures*, Vol. 266, p. 113801, 2021, doi: https://doi.org/10.1016/j.compstruct.2021.113801.

[28] H. Geramizadeh, S. Dariushi, and S. J. Salami, "Optimal Face Sheet Thickness of 3D

Printed Polymeric Hexagonal and Re-entrant honeycomb sandwich beams subjected to three-point bending," *Composite Structures*, vol. 291p. 115618, 2022, doi: https://doi.org/10.1016/j.compstruct.2022.115618.

[29] H. Geramizadeh, S. Dariushi, and S. J. Salami, "Numerical and Experimental Investigation for Enhancing the Energy Absorption Capacity of the Novel Three-dimensional Printed Sandwich Structures," *Proceedings of the Institution of Mechanical Engineers, Part L: Journal of Materials: Design and Applications*, 2021, doi: https://doi.org/10.1177/1464420721997490.

[30] H. Geramizadeh and S. Jedari Salami, "Theoretical, Numerical, and Experimental Investigations of 3D Printed Sandwich Beams Subjected to Three-point Bending," *Iranian Journal of Mechanical Engineering Transactions of ISME*, Vol. 24, No. 2, pp. 134–159, 2022, doi: https://doi.org/10.30506/IJMEP.2022.548520.1856.

[31] I. Maskery, L. Sturm, A.O. Aremu, A. Panesar, C.B. Williams, C.J. Tuck, R.D. Wildman, I.A. Ashcroft, and R.J.M. Hague, "Insights into the Mechanical Properties of Several Triply Periodic Minimal Surface Lattice Structures Made by Polymer Additive Manufacturing," *Polymer*, Vol. 152, pp. 62–71, 2018, doi: https://doi.org/10.1016/j.polymer.2017.11.049.

Appendixes

```
[x, y, z] = meshgrid (-pi:pi/64:pi); % 3D coordinates defined by x, y, z
v = 3*(cos(x)+cos(y)+cos(z))+4*(cos(x).*cos(y).*cos(z)); %Neovius formula
figure(1);
fv=isosurface (x, y, z, v, 0);
hold on;
figure(1);
stlwrite('Neovius_1x1x1.stl',fv);
```
(1)

```
[x, y, z] = meshgrid (-pi:pi/64:pi); % 3D coordinates defined by x, y, z
v=(1.1)*(sin(2*x).*cos(y).*sin(z)+sin(2*y).*cos(z).*sin(x)+sin(2*z).*cos(x).*sin(y))-
0.2*(cos(2*x).*cos(2*y)+cos(2*y).*cos(2*z)+cos(2*z).*cos(2*x))-
0.4*(cos(2*x)+cos(2*y)+cos(2*z)); %Split P formula
figure(1);
fv=isosurface (x, y, z, v, 0);
hold on;
figure(1);
stlwrite('Split_P_1x1x1.stl',fv);
```
(2)

```
[x, y, z] = meshgrid (-pi:pi/64:pi); % 3D coordinates defined by x, y, z
v=(sin(x).*sin(y).*sin(z))+(sin(x).*cos(y).*cos(z))+(cos(x).*sin(y).*cos(z))+(cos(x).*cos
(y).*sin(z)); %Schwarz D formula
figure(1);
fv=isosurface (x, y, z, v, 0);
hold on;
figure(1);
stlwrite('schwarz_D_1x1x1.stl',fv);
```
(3)